Quantitative Surface Raman Spectroscopy of Physisorbed Monolayers on Glassy Carbon

Mark R. Kagan and Richard L. McCreery*

Department of Chemistry, The Ohio State University, 120 West 18th Avenue, Columbus, Ohio 43210

Received April 10, 1995. In Final Form: July 21, 1995[⊗]

Efficient spectrometer design and low-noise CCD detectors permit acquisition of Raman spectra from monolayers of adsorbates on carbon surfaces, particularly glassy carbon (GC). Raman spectra of monolayers of β-carotene, rhodamine 6G, bis(4-methylstyryl)benzene (BMB), and the laser dye BPBD on GC were acquired for the first time. By using GC Raman scattering as an internal standard, scattering from the adsorbate was quantitatively related to surface coverage. Adsorption from solutions of varying concentration demonstrated Langmuirian adsorption for all four compounds, thus allowing unambiguous surface coverage determinations. The Raman signal and signal to noise ratio (SNR) depended on the product of the cross section and the surface number density (β_{ads} D_{ads}), and a detection limit (SNR = 3) for this product was determined to be 1.1×10^{-14} sr^{-1} for current instrumental conditions. This value is comparable to that of a monolayer of an unenhanced absorbate such as benzene (6.5×10^{-15} sr^{-1}). The weakest scatterer studied here (BPBD) is not considered to be resonance enhanced at 514.5 nm, and its observable surface Raman features have cross sections 5–10 times that of benzene. The results represent the first observation of Raman scattering from monolayers on carbon surfaces without the benefit of electromagnetic or strong resonance enhancement.

Introduction

Although its wide potential range and structural ruggedness have made glassy carbon an increasingly popular electrode material, its tendency to adsorb organics complicates the detailed analysis of its electrochemical performance. The study of adsorption on glassy carbon has been hindered in the past by a shortage of instrumental techniques sensitive and selective enough to detect and identify adsorbate molecules present at monolayer or lower surface coverages. Raman spectroscopy clearly possesses the required selectivity and molecular information, but its sensitivity is low. Early Raman studies of adsorbates were performed on silica gel substrates[1,2] whose microporous, transparent nature greatly increased the number of molecules sampled by a given optical configuration. Glassy carbon, being nonporous and optically dense, cannot take advantage of this phenomenon.

The discovery of surface-enhanced Raman spectroscopy (SERS) in the late 1970s led to signal enhancements large enough to make the detection of adsorbate monolayers routine.[3-5] Unfortunately, this effect is limited to a small group of specially prepared surfaces[6] that does not include glassy carbon. Doping of glassy carbon surfaces with silver islands has produced enhancements in adsorbate Raman intensity.[7] However, such an experiment raises the question of whether or not it is the entire surface that is being sampled or just the region in close proximity to the silver islands.[8]

Starting with Campion's work in 1982,[9] the development of high quantum efficiency, low-noise multichannel detectors[10] and high-throughput spectrometers led to a large increase in the fraction of the Raman signal that can be collected from a given sample. This has enabled several groups to obtain the Raman spectra of nonresonant adsorbates in the monolayer regime on low surface area substrates that do not support SERS. These surfaces include fused silica,[11] platinum,[12] aluminum,[13,14] silicon,[15-18] nickel,[9] and single crystal silver.[19] The dominant noise source controlling the detection limits in some, if not all, of these examples was the background associated with the substrate itself.

Raman spectroscopy has been applied extensively to sp^2 carbon materials,[20] with particular emphasis on the effects of microstructure, crystallite size, and intercalation. Since the sampling depth for typical Raman probes of carbon is 100–300 Å, the response is dominated by "bulk" rather than surface structure. Such information has been valuable for correlating carbon structure with electro-

* Author to whom correspondence should be addressed. E-mail: Mccreery.2@osu.edu.

[⊗] Abstract published in *Advance ACS Abstracts,* September 15, 1995.

(1) Hendra, P. J.; Loader, E. J. *Trans. Faraday Soc.* **1971**, *67*, 828–40.
(2) Howe, M. L.; Watters, K. L.; Greenler, R. G. *J. Phys. Chem.* **1976**, *80*, 382–5.
(3) Yamamoto, Y.; Nishihara, H.; Aramaki, K. *J. Electrochem. Soc.* **1993**, *140*, 436–43.
(4) Garoff, S.; Sandroff, C. J. *J. Phys. Colloq.* **1983**, *C10*, 483–6.
(5) Knoll, W.; Philpott, M. R.; Golden, W. G. *J. Chem. Phys.* **1982**, *77*, 219–25.
(6) Birke, R. J.; Lombardi, J. R. In *Spectroelectrochemistry: Theory and Practice*; Gale, R. J., Ed.; Plenum Press: New York, 1988; pp 263–344.
(7) Rubim, J. C.; Kannen, G.; Schumacher, D.; Duennwald, J.; Otto, A. *Appl. Surf. Sci.* **1989**, *37*, 233–43.
(8) Alsmeyer, Y. W.; McCreery, R. L. *Anal. Chem.* **1991**, *63*, 1289–95.
(9) Campion, A.; Brown, J. K.; Grizzle, V. M. *Surf. Sci. Lett.* **1982**, *115*, L153–58.
(10) Epperson, P. M.; Sweedler, J. V.; Bilhorn, R. B.; Sims, G. R.; Denton, M. B. *Anal. Chem.* **1988**, *60*, 327A.
(11) Murray, C. A.; Dierker, S. B. *J. Opt. Soc. Am.* **1986**, *3*, 2151–9.
(12) Pettinger, B.; Friedrich, A.; Tiedemann, U. *J. Electroanal. Chem.* **1990**, *280*, 49–59.
(13) Meier, M.; Carron, K. T.; Fluhr, W.; Wokaun, A. *Appl. Spectrosc.* **1988**, *42*, 1066–72.
(14) Tsang, J. C.; Avouris, P. H.; Kirtley, J. R. *J. Electron Spectrosc. Relat. Phenom.* **1983**, *29*, 343–8.
(15) Perry, S. S.; Campion, A. *J. Electron Spectrosc. Relat. Phenom.* **1990**, *54/55*, 933–42.
(16) Dierker, S. B.; Murray, C. A.; Legrange, J. D.; Schlotter, N. E. *Chem. Phys. Lett.* **1987**, *137*, 453–7.
(17) Hines, M. A.; Harris, T. D.; Harris, A. L.; Chabal, Y. J. *J. Electron Spectrosc. Relat. Phenom.* **1993**, *64/65*, 183–91.
(18) Shannon, C.; Campion, A. *Surf. Sci.* **1990**, *227*, 219–23.
(19) Hallmark, V. M.; Campion, A. *J. Chem. Phys.* **1986**, *84*, 2933–41.
(20) Wang, Y.; Alsmeyer, D. C.; McCreery, R. L. *Chem. Mater.* **1990**, *2*, 557–63.

0743-7463/95/2411-4041$09.00/0

chemical behavior and has provided insight into the mechanisms controlling surface reactivity. However, the only cases where Raman spectra have been obtained from monolayers on carbon have involved strongly resonance enhanced adsorbates, such as rhodamine 6G and metal phthalocyanines.[21]

The objective of the current effort is to exploit recent instrumental advances to extend surface Raman spectroscopy to weaker Raman scatterers adsorbed to sp^2 carbon surfaces such as glassy carbon. The observation of nonresonant scatterers at monolayer levels should greatly increase the generality of surface Raman spectroscopy. In addition, it should provide insight into both the nature of the adsorbate/substrate interaction and its effect on both the vibrational and electronic properties of the adsorbate.

Theory

Using the terminology presented in previous derivations,[22,23] the Raman scattering is given by eq 1:

$$S = P_D \beta D_a \Omega A_D T Q K t \tag{1}$$

where S is the signal measured at the CCD detector (electrons) integrated over the width of the Raman line, P_D is the laser power density (photons s^{-1} cm^{-2}), β is the differential Raman scattering cross section (cm^2 $molecule^{-1}$ sr^{-1}), D_a is the number density of the analyte (molecules cm^{-3}), Ω is the collection angle of the spectrometer measured at the sample (sr), A_D is the sample area monitored by the spectrometer (cm^2), T is the spectrometer transmission (unitless), Q is the detector quantum efficiency (electrons $photon^{-1}$), and t is the measurement time (s). K is a factor which depends on sampling geometry, and the product D_a A_D K is the number of molecules in the sampled region. For an adsorbate, D_{ads} has units of molecules cm^{-2} and $K = 1$, resulting in eq 2:

$$S_{ads} = P_D \beta_{ads} D_{ads} \Omega A_D T Q t \tag{2}$$

Surface enhancement, if present, would increase the effective P_D through enhancement of the local electric field (EM field enhancement) or β_{ads} through adsorbate/substrate interactions (chemical enhancement). The optical properties of GC do not support EM field enhancement, so the adsorbate Raman signal will be proportional to $\beta_{ads}D_{ads}$, the product of the cross section and the surface number density.

For a transparent species observed in solution with 180° backscattered geometry, D_a has units of molecules cm^{-3}, and $K = b$, the monitored path length of the laser beam in the sample, as noted in eq 3:

$$S_{sol} = P_b \beta (D_{vol} b) \Omega A_D T Q t \tag{3}$$

Note that the $D_{vol}b$ product has the same units as D_{ads}, molecules cm^{-2}. Cross sections for nonabsorbing materials may be determined by comparison to an internal standard with a known cross section, via eq 4:

$$\beta_1 = \frac{S_{sol}^{(1)}}{S_{sol}^{(2)}} \beta_2 \frac{D_{vol}^{(2)}}{D_{vol}^{(1)}} \tag{4}$$

For example, if an unknown and benzene are dissolved in a common solvent, the known cross section for the benzene 992 cm^{-1} band,[24] 2.86×10^{-29} cm^2 sr^{-1} $molecule,^{-1}$ can be used to determine the unknown cross section. This approach is accurate for absorbing scatterers provided that the concentration is low enough that the laser and Raman light are not significantly attenuated over the path length involved.

For glassy carbon observed in backscattered mode, Raman scattering occurs from a thin layer at the surface, determined by the laser penetration depth and photon escape depth.[8,25,26] K becomes an effective path length, or sampling depth, equal to $(\alpha_L + \alpha_R)^{-1}$ where

$$\alpha_L = \frac{4\pi k_L}{\lambda_L} \tag{5}$$

$$\alpha_R = \frac{4\pi k_R}{\lambda_R} \tag{6}$$

k_L and k_R are the imaginary part of the refracture index of GC at the laser and Raman shifted wavelengths, respectively. Combining eqs 5 and 6 with eq 1 yields (7).

$$S_{GC} = \frac{P_D \beta_{GC} D_{GC} \Omega A_D T Q t}{\alpha_L + \alpha_R} \tag{7}$$

The $\beta_{GC}D_{GC}$ $(\alpha_L + \alpha_R)^{-1}$ product may be determined by acquiring a spectrum of GC simultaneously with a known pathlength of benzene and using a ratio of eqs 3 and 7 to yield eq 8.

$$\frac{S_{GC}}{S_{benzene}} = \frac{\beta_{GC} D_{GC}}{\beta_{benzene} D_{benzene} (\alpha_L + \alpha_R) b} \tag{8}$$

For the 180° backscattered geometry, eq 8 will apply for GC and benzene measured under the same conditions, provided that the path length in benzene is short compared to the spectrometer depth of field.

Once the $\beta_{GC}D_{GC}$ $(\alpha_L + \alpha_R)^{-1}$ product is known, the GC Raman signal may be used as an internal standard for quantifying adsorbate scattering. The ratio of adsorbate to GC scattering corrects for any variation in $(P_D \Omega A_D Q t)$ provided that the layer of adsorbate does not significantly attenuate the laser or Raman light. The ratio of S_{ads}/S_{GC} can thus be used to determine $\beta_{ads}D_{ads}$ via eq 9.

$$\beta_{ads} D_{ads} = \frac{S_{ads} \beta_{GC} D_{GC}}{S_{GC} (\alpha_L + \alpha_R)} \tag{9}$$

If D_{ads} can be measured or estimated by another means, β_{ads} may be determined.

Finally, Langmuir adsorption isotherms follow the behavior of eq 10 [27]

$$\frac{D_{ads}}{D_{ads}^{\circ}} = \frac{K_{ads} C}{1 + K_{ads} C} \tag{10}$$

where D_{ads}° is the saturation coverage (mol cm^{-2}), C the solution concentration, and K_{ads} the adsorption equilibrium

(21) Palys, B. J.; Puppels, G. J.; Van Den Ham, D.; Feil, D. *J. Electroanal. Chem.* **1992**, *326*, 105–12.
(22) Fryling, M.; Frank, C. J.; McCreery, R. L. *Appl. Spectrosc.* **1993**, *47*, 1965–74.
(23) McCreery, R. L. In Laserna, J. J., Ed. *Modern Techniques in Raman Spectroscopy*; Wiley: New York, in press.
(24) Abe, N.; Wakayama, M.; Ito, M. *J. Raman Spectrosc.* **1977**, *6*, 38.
(25) Ishida, H.; Fukuda, H.; Katagiri, G.; Ishitani, A. *Appl. Spectrosc.* **1986**, *40*, 322–30.
(26) Wada, N.; Solin, S. A. *Physica* **1981**, *105B*, 353–6.
(27) Atkins, P. W. *Physical Chemistry*; Oxford University Press: Oxford, Great Britain, 1978, pp 942–945.

Table 1. Correlation of Solution Phase Raman Scattering Cross Sections with Surface Signal Intensities

compound	band (cm^{-1})[a]	β_{SOL}[b]	$(S_{ads}/S_{GC})_0$[c,d]	K_{ads} (M^{-1})
R6G	773		0.12	
	1184		0.20	1.7×10^5
	1647		0.41	
β-carotene	1005	2.2×10^{-24}	0.098	
	1158	5.6×10^{-24}	0.27	4.7×10^3
	1522	1.1×10^{-23}	0.79	
BMB	1178	1.9×10^{-27}	0.0064	1.4×10^4
BPBD	1000	3.7×10^{-28}	0.0013	1.5×10^2

[a] These band positions are determined from the solution phase spectra. Some of the adsorbate bands show slight shifts relative to these positions. [b] The units for β_{SOL} are cm^2 molecule^{-1} sr^{-1}. [c] $(S_{ads}/S_{GC})_0$ is the value of (S_{ads}/S_{GC}) measured at the isotherm plateau. [d] S_{GC} is the peak area of the glassy carbon 1582 cm^{-1} band, divided by integration time and laser power.

constant. Combining with eq 9 and rearranging yields (11)

$$\frac{S_{ads}}{S_{GC}} = \frac{(S_{ads}/S_{GC})^\circ K_{ads} C}{1 + K_{ads} C} \tag{11}$$

where $(S_{ads}/S_{GC})^\circ$ refers to saturation coverage.

Experimental Section

Tokai GC-20 glassy carbon was prepared by conventional polishing with either 1 μm or 0.05 μm alumina followed by sonication in Nanopure (Barnstead) water to remove any polishing debris. Adsorption was achieved by immediate transfer of the polished glassy carbon into the analyte solution of interest for a fixed period of time (typically 5–10 min), followed by a fast rinse (~10 s) in the same solvent used to make the solution. The adsorbates studied were Rhodamine 6G (R6G, Lambda Physik), 1,4-bis(2-methylstyryl)benzene (BMB, Aldrich), β-carotene (Sigma), and 2-(4-biphenylyl)-5-(4-*tert*-butylphenyl)-1,3,4-oxadiazol (BPBD-365, Exciton). The solvents used were reagent grade acetone, anhydrous methanol, carbon tetrachloride, acetonitrile, and methylene chloride.

The Raman spectra were acquired with 514.5 nm excitation and an epi-illuminated, 180° backscattered collection geometry. A detailed description of the spectroscopic apparatus can be found in a previous publication.[28] The focusing and collection lens was either a *f*/4 singlet (focal length = 120 mm) or a *f*/1.4 camera lens (focal length = 50 mm). The greater collection efficiency provided by the camera lens helped to reduce the integration time that was needed to obtain signals with adequate SNR from adsorbed BMB and BPBD. The camera lens was avoided when the R6G and β-carotene adsorbate spectra were acquired, because its tighter focus and higher power density caused photodegradation of β-carotene and R6G. This observation illustrates an example of sensitivity limited by sample radiation damage. The *f*/1.4 lens yields a larger signal but a higher laser power density. Since the resonant scatterers are more prone to photodegradation, they required the less sensitive *f*/4 lens with its accompanying lower power density and collection efficiency.

Solution cross sections were determined by comparing integrated peak areas for dilute solutions of each of the four materials with that of the 992 cm^{-1} band of benzene dissolved in CCl_4, via eq 4. Solution cross sections are listed in Table 1, except for R6G, which was too fluorescent to observe Raman features. The $\beta_{GC} D_{GC} (\alpha_L + \alpha_R)^{-1}$ product for GC was determined by comparison to a 1 mm path length of benzene via eq 8. A long focal length (500 mm) lens assured a long depth of field (>5 mm), and the GC and benezene samples were positioned identically in the beam.

The cyclic voltametric measurements of 2,6-anthraquinonedisulfonate (AQDS) adsorption were performed in a three-electrode cell with polished glassy carbon as the working electrode, Ag/AgCl as the reference electrode, and platinum as the auxiliary electrode. The supporting electrolyte was 0.2 M perchloric acid, and the scan rate was 2 V/s. The voltametry was performed in the same solution from which AQDS adsorption occurred. All experiments were performed in ambient atmospheric conditions.

(28) Kagan, M. R.; McCreery, R. L. *Anal. Chem.* **1994**, *66*, 4159–65.

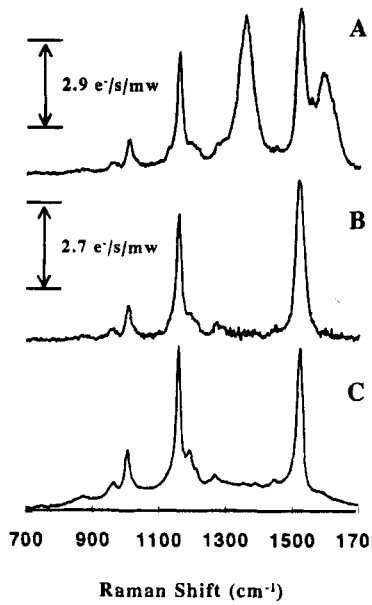

Figure 1. (A) Raman spectrum of β-carotene adsorbed on polished glassy carbon from a 10.5 mM solution in methylene chloride. The glassy carbon was submerged for 5 min in the solution before being removed and rinsed with pure methylene chloride. The excitation wavelength was 514.5 nm, the laser power was 10 mW at the sample, and the integration time was 60 s with an *f*/4 collection lens. (B) Same as previous except that the glassy carbon spectrum has been subtracted. (C) Raman spectrum of a 3.1 μM solution of β-carotene in carbon tetrachloride after solvent subtraction: 514.5 nm, 20 mW, 5 s integration.

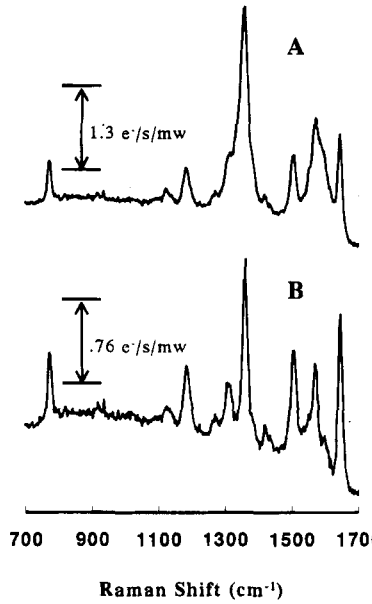

Figure 2. (A) Raman spectrum of R6G adsorbed to glassy carbon from a 1.14 mM solution in methanol. The glassy carbon was submerged for 5 min in the solution before being removed and rinsed with pure methanol: 514.5 nm, 15 mW, 180 s integration time, *f*/4 lens. (B) Same as A except that the glassy carbon spectrum has been subtracted.

Results

Figures 1–4 show the Raman spectra of β-carotene, R6G, BMB, and BPBD adsorbed to glassy carbon (A), adsorbed to glassy carbon with the glassy carbon bands subtracted (B), and dissolved in solution with the solvent

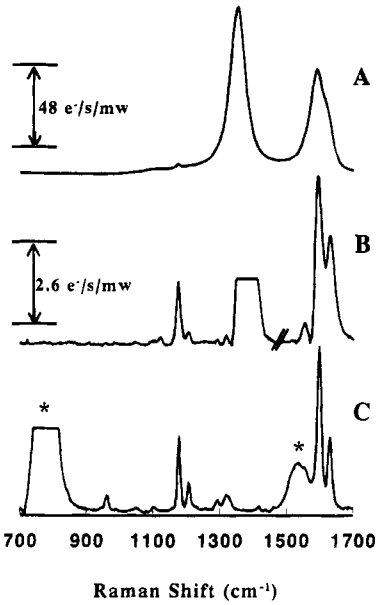

Figure 3. (A) Raman spectrum of BMB adsorbed to glassy carbon from acetone. This spectrum is the average of 18 individual spectra in which the solution concentrations ranged from 0.57 to 5.7 mM. For each of the individual spectra, the glassy carbon was submerged for 10 min in the solution before being removed and rinsed with pure acetone: 514.5 nm, 10 mW, 2520 s total integration time, *f*/1.4 lens. (B) Same as previous except that the glassy carbon spectrum has been subtracted. (C) Raman spectrum of a 1.0 mM solution of BMB in carbon tetrachloride after solvent subtraction: 514.5 nm, 20 mW, 5 s integration time.

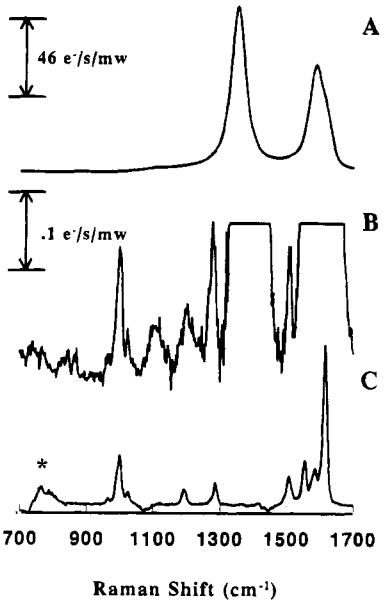

Figure 4. (A) Raman spectrum of BPBD adsorbed to glassy carbon from an 11 mM solution in acetonitrile. The glassy carbon was submerged for 10 min in the solution before being removed and rinsed with pure acetonitrile: 514.5 nm, 50 mW, 3600 s integration time, *f*/1.4 lens. (B) Same as previous except that the glassy carbon spectrum has been subtracted out. (C) Raman spectrum of a 10 mM solution of BPBD in carbon tetrachloride after solvent subraction: 514.5 nm, 20 mW, 5 s integration time.

bands subtracted (C). It will be shown that the adsorbate spectra in these figures represent surface coverages in the monolayer regime. Overall, the adsorbate signals (indicated by S_{ads}/S_{GC} in Table 1) track the magnitudes of the solution phase cross sections. The Raman spectra of R6G and β-carotene were resonantly enhanced by the 514.5 nm excitation employed. This resulted in strong adsorbate bands that are clearly visible, even before subtraction of the glassy carbon background. The Raman spectra of BMB and BPBD were not resonantly enhanced by the 514.5 nm excitation, resulting in much weaker adsorbate bands that only become visible after subtraction of the glassy carbon background. In the case of BPBD, the weakest of the Raman scatterers studied, the adsorbate bands were nearly 500 times smaller than the glassy carbon bands. A comparison of the β-carotene, BMB, and BPBD adsorbate spectra with their respective solution phase spectra shows a strong correlation with respect to band positions. Peak frequency changes upon adsorption were quite small (<3 cm^{-1}) and do not permit structural conclusions at this time. However, both BMB and BPBD adsorbate spectra show some significant intensity changes relative to their solution phase spectra. In fact, the BMB and BPBD solution phase Raman bands at 963 and 1194 cm^{-1}, respectively, appear to be completely absent in the corresponding adsorbate spectra. A solution phase spectrum for R6G could not be obtained due to excessive fluorescence interference. The fluorescence quenching ability of the glassy carbon surface permitted the acquisition of the R6G adsorbate spectrum.[28]

In the spectral region covered in these studies, glassy carbon has two major bands. Subtraction of these bands was complicated by the fact that their intensity ratio varied slightly from sample to sample, most likely due to small variations in polishing that were difficult to control. This led to an incomplete subtraction of the glassy carbon bands that is clearly visible in Figures 3B and 4B. The discontinuity at approximately 1470 cm^{-1} in spectrum 3B indicates that the glassy carbon spectrum that was subtracted from the right-hand portion of spectrum 3A was scaled by a slightly different factor than the glassy carbon spectrum that was subtracted from the left-hand portion of spectrum 3A. It was necessary to do this in order to reveal all of the adsorbed BMB spectral features.

When discussing Raman signals, S_{ads} will indicate the integrated area above baseline (e^-) of an absorbate Raman feature, divided by the laser power and integration time, with units of $e^- s^{-1} mW^{-1}$. This quantity compensates for variations in laser power and/or integration time. Figure 5 shows plots of (S_{ads}/S_{GC}) versus the solution concentration present during adsorption for R6G, β-carotene, BMB, and BPBD, where S_{ads} and S_{GC} are the Raman signal intensities of the adsorbate and the glassy carbon, respectively. The adsorbate Raman intensity was determined for a peak which was separated from the carbon Raman features, but all adsorbate peaks show similar trends. The experimental data is represented by the solid circles, and the curves represent the best fit of the experimental data to a Langmuir isotherm (eq 11). The quality of the fits are indicated by R^2 values of 0.99, 0.99, 0.96, and 0.98 for R6G, β-carotene, BMB, and BPBD, respectively. Clearly, the results are consistent with Langmuirian adsorption, and the plateau region indicates the conditions required for monolayer coverage. The adsorbate spectra in Figures 1–4 were all acquired from samples exhibiting saturation coverage on the plateau of the isotherms. The signals at saturation coverage and the adsorption equilibrium constants derived from the isotherms are listed in Table 1.

The ratio (S_{ads}/S_{GC}) was used instead of S_{ads} in all of the isotherms in order to correct for variations in collection efficiency, power density, etc. In the case of BMB and BPBD, where the adsorbate Raman bands were so small that they did not interfere with the glassy carbon Raman bands, both adsorbate and glassy carbon Raman signals were measured from the same spectrum. In the case of R6G and β-carotene, where the adsorbate Raman bands

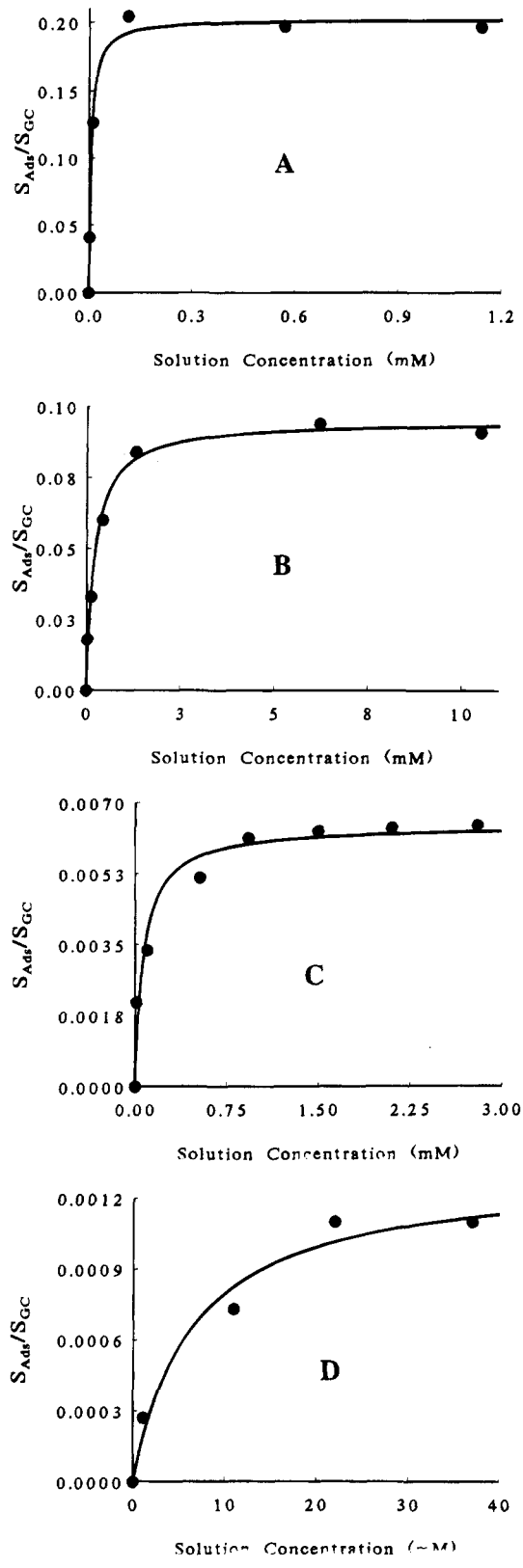

Figure 5. Plots of the ratio of integrated adsorbate to glassy carbon Raman signal intensity versus concentration in the adsorption solution. The circles represent experimental data while the solid lines represent the best fits to eq 11. The glassy carbon Raman signal monitored in all cases was the 1582 cm^{-1} band integrated over its entire width. (A) R6G from methanol, 1184 cm^{-1} Raman band. (B) β-carotene from methylene chloride, 1005 cm^{-1} Raman band. (C) BMB from acetone, 1178 cm^{-1} Raman band. (D) BPBD in acetonitrile 1000 cm^{-1} Raman band. In all cases the adsorbate Raman bands were integrated over their entire widths.

were large enough to obscure the glassy carbon Raman bands, the adsorbate and glassy carbon Raman signals were measured separately, on the same day under identical conditions.

The amount of BMB adsorption to glassy carbon resulting from a 10 min submersion in a 1 μM solution was compared with the amount of adsorption that occurred from a 20 h submersion in the same solution. There was no significant difference. A 1 μM concentration was chosen because it represented the most dilute solution used in these experiments. This result indicates that the isotherms of Figure 5 were obtained under equilibrium conditions.

All adsorbate Raman spectra were acquired after the glassy carbon was removed from the solution and rinsed, to reduce the possibility of spectral interference from the solvent and unabsorbed analyte. The purpose of the solvent rinse was to remove the layer of solution that was unavoidably transferred along with the glassy carbon. In all cases the rinsing time was limited to 10 s or less in order to avoid significant washing away of the adsorbate. The amount of adsorbate removed by the 10 s rinse was estimated by measuring the adsorbate Raman signal intensity for a series of rinsing times ranging from a few seconds to 30 min and then extrapolating the results to $t = 0$. The difference between the adsorbate Raman signal intensity at $t = 0$ and the 10 s rinse indicates that for R6G, β-carotene, BMB, and BPBD, the amount of adsorbate removed by the 10 s rinse was less than 1% of the total. For example, the Raman signal for adsorbed BMB decreased by 30% while standing for 30 min in acetone.

The quantity $\beta_{GC}D_{GC}(\alpha_L + \alpha_R)^{-1}$ was determined via eq 8 for several slit widths (to vary A_D and resolution) and focal lengths (to vary depth of field). For the 1360 cm^{-1} band of polished GC excited by a 514.5 nm laser, $\beta_{GC}D_{GC}(\alpha_L + \alpha_R)^{-1}$ averaged 1.13×10^{-10} sr^{-1} (range $(1.11-1.15) \times 10^{-10}$ sr^{-1}) for slit widths of 25 to 100 μm and collection lens focal lengths of 25 and 50 cm. Although this result may vary with GC source and preparation, its constancy with instrumental variables indicates that it is reliable for the GC surfaces studied here. The value of $\beta_{GC}D_{GC}(\alpha_L + \alpha_R)^{-1}$ determined for the 1582 cm^{-1} band of glassy carbon using eq 8 was 7.7×10^{-11} sr^{-1}. The validity of this approach was assessed by using it to calculate the same quantity for the 1582 cm^{-1} band of highly ordered pyrolytic graphite (HOPG), yielding a value of $\beta_{HOPG}D_{HOPG}(\alpha_L + \alpha_R)^{-1}$ of 3.3×10^{-11} sr^{-1}. Using a different approach, Wada and Solin[26] determined the same quantity for HOPG and obtained a value that ranged between 4.3×10^{-11} sr^{-1} and 5.4×10^{-11} sr^{-1}, depending on the literature values of α_L and α_R used. It should be noted that the values of α_L and α_R for HOPG are different from the values for glassy carbon.

Finally, the effect of surface roughness on the Raman signal intensity of adsorbates was examined by a comparison of spectra from GC polished with 0.05 μm alumina vs 1.0 μm alumina, with the results shown in Table 2. They indicate that the surface coverage of adsorbed 2,6-anthraquinonedisulfonate (AQDS), determined by cyclic voltametry,[29] was greater than twice as large for the 1 μm polished glassy carbon as it was for the 0.05 μm polished glassy carbon. The results also indicate that this increase in microscopic surface area did not result in a corresponding increase in the Raman signal of adsorbed R6G.

Discussion

Table 3 lists the $\beta_{ads}D_{ads}$ products at saturation coverage, determined from eq 9. The $\beta_{ads}D_{ads}$ product varies by a

(29) McDermott, M. T.; Kneten, K.; McCreery, R. L. *J. Phys. Chem.* **1992**, *96*, 3124–30.

Table 2. Microscopic Surface Area Measured by Cyclic Voltammetry and Its Effect on Adsorbate Raman Signal Intensity

	0.05 μm polish[a]	1 μm polish[a]	1 μm/0.05 μm
Γ_{AQDS} (10 μM)[b]	93.8	225	2.40
Γ_{AQDS} (30 μM)	160	383	2.39
Γ_{AQDS} (60 μM)	148	348	2.35
S_{R6G}/S_{GC} (1.5 mM)[c]	0.20	0.23	1.15

[a] 0.05 μm polish and 1 μm polish refer to glassy carbon polished with 0.05 μm and 1 μm alumina particles. [b] Γ_{AQDS} is the surface coverage of AQDS in pmol/cm^2 as measured by cyclic voltammetry in a solution with the indicated AQDS concentration. [c] S_{R6G}/S_{GC} is the integrated area of the 1184 cm^{-1} Raman band of adsorbed R6G divided by the integrated area of the 1582 cm^{-1} Raman band of glassy carbon. The R6G solution concentration during adsorption was 1.5 mM.

Table 3. Raman Scattering Cross Sections of Molecules Adsorbed to a Glassy Carbon Surface, 514.5 nm Excitation

compound	band (cm^{-1})	$\beta_{ads}D^{\circ}_{ads}$[a]	D°_{ads}[b]	β_{ads}[c]	β_{ads}/β_{sol}
R6G	773	9.2×10^{-12}	7.2×10^{13}	1.3×10^{-25}	
	1184	1.5×10^{-11}		2.1×10^{-25}	
	1647	3.2×10^{-11}		4.4×10^{-25}	
β-carotene	1005	7.5×10^{-12}	4.6×10^{13}	1.6×10^{-25}	0.073
	1158	2.1×10^{-11}		4.6×10^{-25}	0.082
	1522	6.1×10^{-11}		1.3×10^{-24}	0.12
BMB	1178	4.9×10^{-13}	7.2×10^{13}	6.8×10^{-27}	3.6
BPBD	1000	1.0×10^{-13}	8.4×10^{13}	1.2×10^{-27}	3.2

[a] The units of $\beta_{ads}D_{ads}$ are sr^{-1}. [b] Determined by assuming a flat, close packed monolayer, in molecules cm^{-2}. [c] The units of β_{ads} are cm^2 molecule^{-1} sr^{-1}.

factor of 600 for the four adsorbates studied, with the weakest feature reported having a value of 1.0×10^{-13} sr^{-1}. For comparison, a monolayer of benzene on a flat surface has a βD product of 6.5×10^{-15} sr^{-1} for its strongest Raman band. The optical properties of GC are not amenable to the electromagnetic field enhancement observed on SERS active metals, at least in the visible wavelength region.[6] BPBD exhibits a solution phase cross section comparable to similar molecules in the absence of resonance enhancement and would be considered weakly resonant if at all. The spectra of BPBD in Figure 4 would therefore be considered "unenhanced" by either EM field enhancement or resonance Raman enhancement. The decrease in signal to noise ratio (SNR) in progressing to weaker scatterers (Figures 1–4) clearly demonstrates the importance of the magnitude of $\beta_{ads}D_{ads}$ and the integration time to obtaining surface spectra.

The value of D°_{ads} for the four adsorbates at monolayer coverage was estimated through use of the HyperChem molecular simulation program (Autodesk, Inc). A tightly packed, flat geometry was assumed for the estimates. These results are tabulated in the fourth column of Table 3. The fifth column of Table 3 lists the values of β_{ads} calculated from $\beta_{ads}D^{\circ}_{ads}$ and D°_{ads}. To our knowledge, these are the first reported Raman scattering cross sections for molecules adsorbed on a carbon substrate. The final column of Table 3 shows a comparison of these values with the corresponding solution phase values in Table 1. Notice that there is a small enhancement (<5-fold) in the BMB and BPBD Raman scattering cross sections upon adsorption In constrast, there is a decrease (about 14-fold) in the adsorbed β-carotene Raman scattering cross section. It is interesting to note that the results for BMB and BPBD are similar to those of Sakamoto et al. who also found an approximate 4-fold increase in the cross section of nitrobenzene adsorbed on Ni(111) compared to liquid nitrobenzene.[30] Given the optical properties of GC, an electromagnetic field enhancement such as that observed in SERS would not be expected. A polarizability change upon adsorption ("chemical enhancement") is possible and may underlie the increase in β_{ads} for BMB and BPBD. The decrease in β_{ads} for the resonance-enhanced β-carotene may result from an electronic interaction between the adsorbate and the carbon surface. An electronic interaction between the two conjugated systems might shift the absorption spectrum of the β-carotene, thus changing the degree of resonance enhancement. Such an effect would be revealed by determining β_{ads} for several laser wavelengths, which is currently in progress.

The general signal to noise (SNR) expression for a Raman spectroscopic analysis is given by eq 12.

$$\mathrm{SNR} = \frac{St^{1/2}}{(S + B + D + \sigma_R{}^2)^{1/2}} \tag{12}$$

where S is the height of the analyte peak (electrons s^{-1}), B is the height of the background below the analyte peak (electrons s^{-1}), D is the dark signal (electrons s^{-1}), σ_R is the readout noise (electrons), and t is the measurement time (s). For the 998 cm^{-1} band of adsorbed BPBD shown in Figure 4B, S equals 6.5 electrons s^{-1} and B equals 120 electrons s^{-1}, for a measurement time of 3600 s. For the CCD detector used to acquire this spectrum, D and σ_R are negligible compared to B and can be ignored in eq 12. S can also be ignored in the denominator as well due to its small magnitude relative to B. The resulting SNR expression for this example reduces to the background shot noise limit, eq 13.

$$\mathrm{SNR} = \frac{St^{1/2}}{B^{1/2}} \tag{13}$$

Equation 13 predicts a SNR of 36 for the 998 cm^{-1} band of adsorbed BPBD for $S = 6.5$ e$^-$ s^{-1}, $B = 120$ e$^-$ s^{-1} and $t = 3600$ s. The observed value of 33 from Figure 4B indicates that the measurement is occurring at the background shot noise limit.

Equations 12 and 13 indicate that the glassy carbon background signal is the dominant noise source in the Raman spectra of adsorbates with weak scattering cross sections. Greatly improved detection limits would result from a reduction in this background. Our experiments indicate that this background is due to a broad band inelastic scattering process or fluorescence. Instrumental improvements can partially alleviate this problem (by increasing $A_D\Omega TQ$), but ultimately the SNR will be limited by carbon background.

For the background shot noise limited case, inspection of eqs 13 and 1 reveals that the SNR is proportional to $\beta_{ads}D_{ads}$. On the basis of the observed GC background, one can predict the minimum $\beta_{ads}D_{ads}$ product which can be detected with an SNR = 3. For 10 mW of laser power at the sample, $t = 3600$ s, and the spectrometer employed here, $(\beta_{ads}D_{ads})_{min} = 4.1 \times 10^{-14}$ sr^{-1} for the $f/4$ singlet lens and 1.1×10^{-14} sr^{-1} for the $f/1.4$ camera lens. Table 4 illustrates the calculated surface coverages for the four adsorbates at this detection limit. With present technology, surface coverage well under 1% of a monolayer can be detected.

The Langmuir plots shown in Figure 5 and the K_{ads} values in Table 1 can be used to compare the strength of

(30) Sakamoto, K.; Mizutani, G.; Ushioda, S. *Phys. Rev. B* **1993**, *48*, 8993–9005.

Table 4. Predicted Detection Limits for Several Adsorbate Bands

absorbate	band cm^{-1}	collection lens	detection limit, monolayers, for SNR = 3[a]
R6G	773	*f*/4	0.0045
	1184	*f*/4	0.0027
β-carotene	1005	*f*/4	0.0055
	1158	*f*/4	0.002
BMB	1178	*f*/1.4	0.022
BPBD	1000	*f*/1.4	0.11

[a] Power at sample = 10 mW, t = 3600 s,

the adsorption interaction for the various solute-solvent combinations tested.[27] Note that a quantitative knowledge of spectrometer performance or cross sections is unnecessary to calculate K_{ads}. The ability to determine K_{ads} could lead to a better understanding of the molecular features that control the strength of the adsorption interaction on glassy carbon.

The observation that microscopic surface area does not affect the Raman signal intensity of an adsorbed monolayer on glassy carbon can be understood by closer inspection of eq 1. This equation states that the adsorbate Raman signal intensity is proportional to both the laser power density (P_D) and the adsorbate number density (D_{ads}). An increase in microscopic area from surface roughness will increase the number of scatterers in the beam but will proportionately decrease the local power density. Thus, roughness will not change the product $P_D D_{ads}$ or the observed signal, as demonstrated in Table 2. It must be noted that this argument is only valid for a nonporous surface such as the glassy carbon used in these experiments. For an increase in microscopic surface area caused by porosity, P_D does not necessarily decrease since the laser radiation can impinge on more than one surface, provided that the pore diameters and spacing are small relative to the penetration depth of the laser. These arguments are illustrated in Figure 6.

In summary, Raman spectroscopy was used to detect organic monolayers adsorbed to a glassy carbon surface. The adsorbates studied ranged from resonantly enhanced R6G and β-carotene to the nonresonant BPBD. Utilization of the glassy carbon Raman band as an internal standard led to a quantitative correlation between the surface Raman signals and the surface coverage. This allowed adsorption isotherms to be obtained that provided unambiguous surface coverage data. Calibration of the glassy carbon Raman band intensity allowed the surface scattering cross section of several adsorbates to be determined and compared to their solution phase values. Finally, signal to noise ratio and surface area considerations were explored.

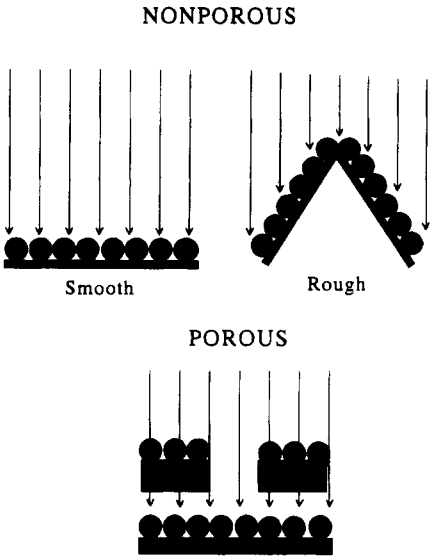

Figure 6. Comparison of porous versus nonporous surfaces. The solid circles represent adsorbate molecules while the arrows represent incoming laser radiation.

Acknowledgment. The authors thank Mark Fryling for valuable contributions to the quantitation of GC scattering. This work was supported by the Analytical and Surface Chemistry Division of the National Science Foundation.

LA9502857